THE JOURNAL OF PHYSICAL CHEMISTRY C

ARTICLE

pubs.acs.org/JPCC

Formation of Arrays of Free-Standing CdS Quantum Dots Using the Langmuir−Blodgett Technique

Dmitry Yu. Protasov,*[,†] Wen-Bin Jian,[‡] Kirill A. Svit,[†] Tatyana A. Duda,[†] Sergei A. Teys,[†] Anton S. Kozhuhov,[†] Larisa L. Sveshnikova,[†] and Konstantin S. Zhuravlev[†]

[†]A.V. Rzhanov Institute of Semiconductor Physics, pr. Lavrentieva, 13, Novosibirsk 630090, Russia

[‡]Department of Electrophysics, NCTU, Hsinchu 30010, Taiwan

ABSTRACT: Aggregation clusters of CdS quantum dots (QDs) on the highly ordered pyrolytic graphite substrate were investigated by atomic force microscopy and scanning tunneling microscopy. QDs were initially formed within Y-type Langmuir−Blodgett (LB) films of cadmium behenate. The LB matrix was then removed by annealing. To study the process of QD assembly, the density of QDs in the initial film was varied systematically by increasing the number of monolayers (MLs) from 1 to 20 ML. It was found that, at a small LB ML number, only a small part of CdS molecules form into QDs by diffusion along the plane of LB layers. With an increase of the LB ML number, the interlayer diffusion arises that leads to almost full binding of CdS molecules into QDs. The individually standing QDs were formed on the substrate for 1 and 2 ML samples. The QD size distributions of the samples with a small ML number are broader than that predicted by the two-dimensional Lifshitz−Slezov diffusion model. With an increase of the LB matrix thickness, QDs begin to assemble into clusters, revealing a ribbon structure due to diffusion-limited aggregation, and for the 20 ML LB matrix, a submonolayer QD film arises. By analyzing the occurrence of QDs as a function of aggregation number, pair bondings were estimated to be about 34 and 62 meV for the 4 and 8 ML samples, respectively.

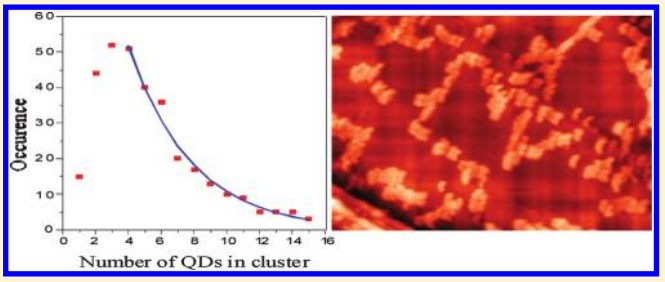

INTRODUCTION

Semiconductor quantum dots (QDs) are promising materials for novel optical and electronic applications due to their new properties, which do not exist in bulk materials. The novel properties of the QDs should be applied to improve the performance of conventional devices and to develop new functional devices. II−IV compound QDs are more attractive materials for development and fabrication of photosensitive and photovoltaic devices, lasers, sensors, optical switches, solar cells, and various biological application devices.[1,2]

Common ways to prepare QDs are molecular beam epitaxy, advanced X-ray and electron-beam lithography, and scanning probe etching techniques. Such methods are sophisticated and expensive and require ultra-high-vacuum equipment and super clean environmental conditions. Another, and the cheapest, method is a chemical approach,[3] including colloidal synthesis and the Langmuir−Blodgett (LB) technique,[4−7] which is adopted in this work. The LB technique is one of the most promising methods for synthesizing PbS, CdS, and ZnS QDs.

For development of device applications, it is frequently necessary to fabricate ordered QD arrays on various substrates. Moreover, such ordered or self-assembled nanostructures show remarkable collective properties different from that of a single QD.[8] This gives an additional opportunity to study the collective physical phenomena in ensembles of the QDs and to design novel devices. Therefore, creating self-assembled QD arrays by using different, novel, and innovative procedures attracts much attention. The process of self-assembly has been actively investigated in the formation of the QD ensembles from colloidal solutions.[9,10] It was shown that the process of clustering strongly depends on the growth time[10−12] and pH value of the solution.[13] The superlattices of semiconductor QDs,[14] magnetic nanoparticles,[15] and metal nanocrystals[16] have been produced using solvent evaporation.

In this paper, preparation processes of CdS QDs by the LB technique and ensembles of QDs by thermally induced desorption of the solid matrix will be reported. The former process corresponds to dissociation of oversaturated CdS molecules in behenic acid solution. This process has been investigated and described in the framework of the Lifshitz−Slezov diffusion model[17] generalized by Nabok et al. for the two-dimensional case.[18] The second process of QD clustering at thermally induced desorption of behenic acid is, in many respects, similar to that taking place at the evaporation of nanoparticles in solvent.[11] Nevertheless, as far as we know, the process of QD assembly on the substrate after removing the LB matrix has not been studied yet.

Received: July 17, 2011
Revised: August 25, 2011
Published: August 31, 2011

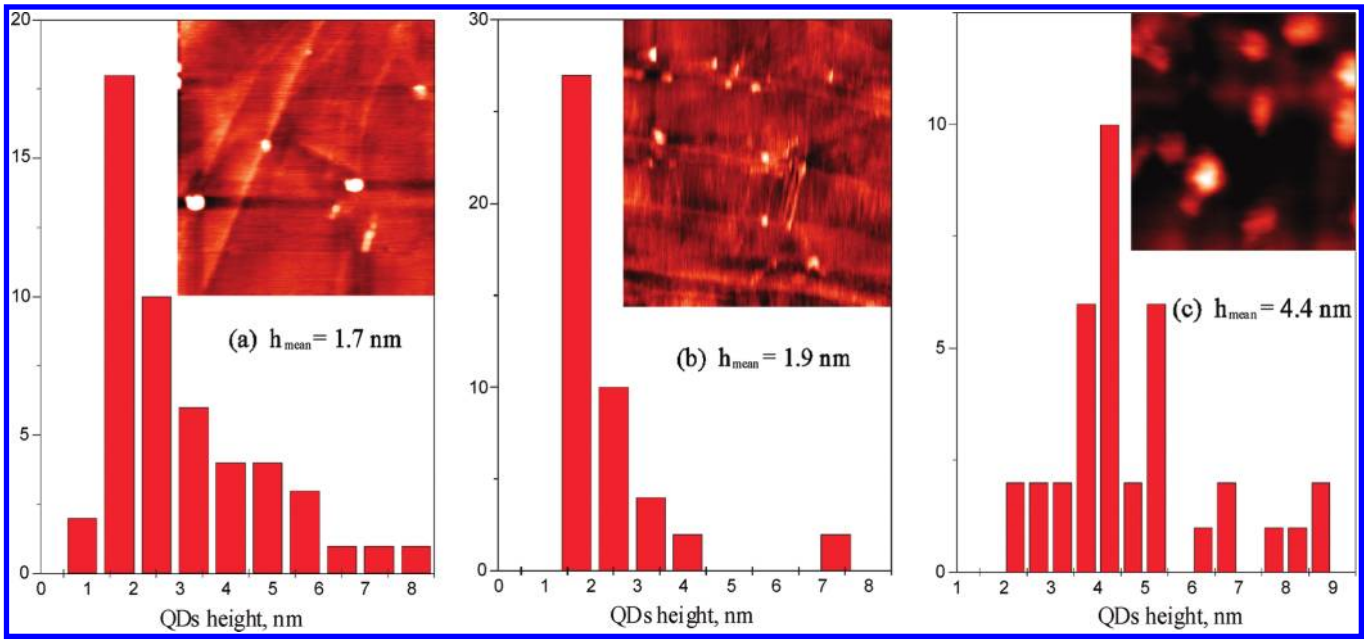

Figure 1. Size distribution of QDs for the 1 (a), 2 (b), and 3 ML (c) samples. The insets show the 1 × 1 μm AFM images.

EXPERIMENTAL SECTION

The samples containing CdS QDs were formed by the LB technique. To study the process of QD assembly, the density of QDs in the investigated samples was varied systematically. The substrate used here was a highly ordered pyrolytic graphite (HOPG). At first, films of cadmium behenate ($CdBh_2$) were prepared by transferring a few monolayers of the salt (1, 2, 3, 4, 8, or 20 ML with a thickness of about 3, 6, 9, 12, 24, and 60 nm, respectively) from the surface of an aqueous subphase containing cadmium chloride onto the substrates. Hereinafter, we will distinguish the samples using the number of the LB monolayers (MLs). The LB MLs were transferred by Y-type deposition at a pressure of 30 mN/m and a temperature of 22 °C. For obtaining an odd ML number, the $CdBh_2$ was removed from the surface of the liquid subphase before the last lift of the substrate. The $CdBh_2$ films were then exposed to a hydrogen sulphide gas at a pressure of 100 Torr for 1.5 h at 22 °C. As a result of the interaction between the cadmium behenate salt and the hydrogen sulphide, the cadmium sulfide QDs distributed inside the behenic acid matrix have appeared. At last, the LB film matrix was removed by thermally induced desorption of the behenic acid in ammonia gas under atmospheric pressure at 200 °C. The procedure of the nanocluster preparation was described in detail earlier.[7]

The CdS QDs were analyzed by atomic force microscopy (AFM) and scanning tunneling microscopy (STM). In the AFM experiments, we used a Solver P-47H (NT MDT) atomic force microscope with a vertical resolution as high as ~0.5 Å. Measurements were performed at room temperature. The STM measurements were performed using an ultra-high-vacuum Omicron AFM/STM at room temperature. STM images of CdS QDs arrays were obtained in a constant current mode with the following scanning parameters: a sample bias (V_b) of 2.5 V and a set-point tunneling current (I_s) in the range between 0.02 and 1.04 nA. Sizes of CdS QDs and QD clusters have been determined using a software for AFM and STM image processing. The density and size of QDs were estimated by visual counting from AFM images in order to exclude errors caused by the roughness of the substrate.

RESULTS AND DISCUSSION

The size distributions of QDs for the 1, 2, and 3 LB ML samples are presented in Figure 1a−c, respectively. In the insets, the 1 × 1 μm AFM images of these samples are shown. The size of a QD is decided by its height that was measured by AFM with a high accuracy. Because of the low density of QDs per square centimeter in the 1−3 LB ML samples, we used a rather large area (3 × 3 μm) of AFM images to obtain the QD height distributions that contains about 50 image data. In the 1 LB ML sample, QDs have a mean size of ~1.7 nm with a density of about 5×10^8 cm^{-2}. Besides, it is observed from the height distribution that the large part of QDs has a large height up to 8 nm. For the 2 LB ML sample, the QD density increases up to 1×10^9 cm^{-2}. In this sample, the mean value of the QDs' height is ~1.9 nm, whereas the QD height deviation is less than that for the 1 LB ML sample. It is seen from the inset to Figure 1c that, in the 3 LB ML sample, QDs aggregate to form arrays, consisting of a few dots with a mean height of about 4.4 nm. The density of QDs in this sample is about 5×10^9 cm^{-2}. As one can see from Figure 1a−c, the relative portion of small QDs decreases with an increase of the LB ML.

The height distributions of QDs differ from the theoretical prediction[18] within the generalized Lifshitz−Slezov diffusion model. This model considers the separation of phases in a many-component system consisting of a minor phase dissolved in a major phase. Deviation from equilibrium in such many-component system initiates a three-staged process: During the initial stage, droplets of a new phase are formed due to fluctuations in concentration of a minor phase; then the droplets grow and absorb impurity atoms from a solution. The last stage of this process is the Ostwald ripening starting when the concentration of the impurity in a solution is close to equilibrium. At this stage, the big droplets grow due to dissolution of smaller ones. It is seen from Figure 1 that the experimental height distributions are

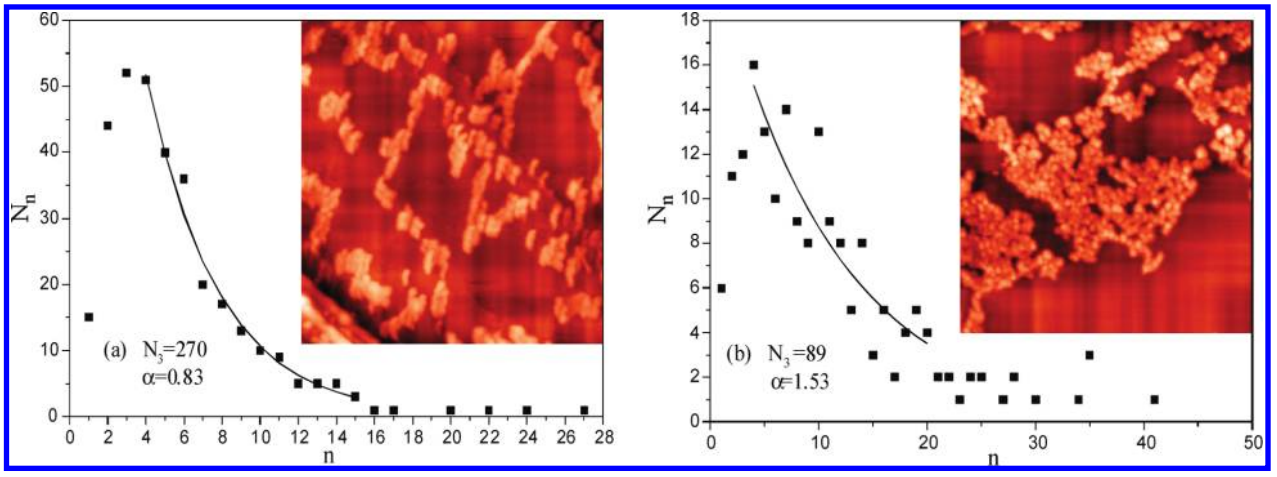

Figure 2. Occurrence as a function of the aggregation number n for the 4 (a) and 8 ML (b) samples. The solid line presents the fitting results. The insets show the 1 × 1 μm AFM images.

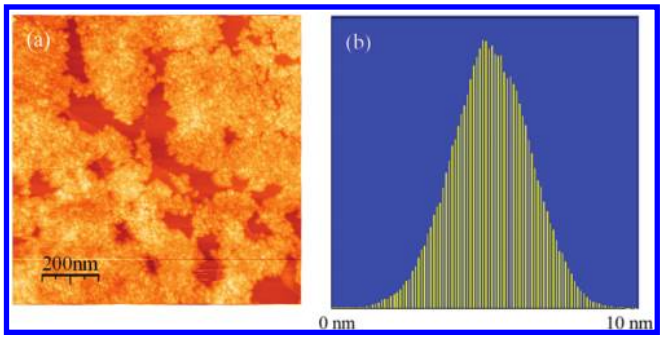

Figure 3. STM image of the 20 ML sample with the QD concentration of 1×10^{12} cm^{-2} (a). The QDs' size distribution with a mean height size of 5.5 nm (b).

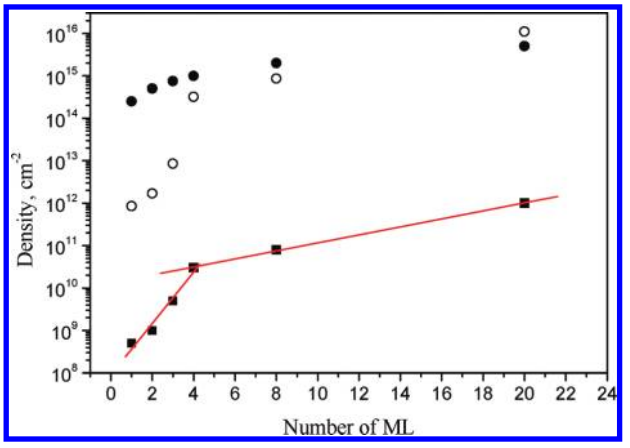

Figure 4. Dependencies of the density of QDs (■), CdS molecules in the LB matrix (●), and CdS molecules in QDs (○) on the ML number. The linear fit for the QD density is represented by the solid red line.

expanded and the QDs grow to bigger ones, while the theory predicts a very fast decrease of the QD density with size r larger than a critical radius r_{cr} and the QD density is close to zero for $r \approx 3/2r_{cr}$. This divergence may be explained since the generalized Lifshitz−Slezov diffusion model is valid for a very small volume fraction ϕ of the minority phase. The thickness of 1 ML after sulphidation and QD formation in the LB films increases approximately by 7%,[19] so the fraction of the minority phase does not exceed 10%. Yao et al.[20] show that the distribution function is very sensitive to the ϕ value and the full width at half-maximum (fwhm) of the distribution function rises twice at increase ϕ from ~0 to 10%. We suggest that the QD height distributions can be explained by a more accurate theoretic model describing a 2D diffusion of CdS molecules along the LB MLs and a 3D growth of spherical QDs at large ϕ values.

In the insets to Figure 2a,b, the AFM images for the 4 and 8 LB ML samples are shown. These data evidence that, at the further increase of the ML number, the average density of QDs sharply increases up to 3×10^{10} cm^{-2} for the 4 LB ML sample, and to 8×10^{10} cm^{-2} for the 8 LB ML sample. The occurrence number (N_n) as a function of the QD aggregation number (n) will be discussed later.

Figure 3a,b shows the STM image of the 20 LB ML sample, and the QD height distribution was obtained through the histogram analysis of the image data using the image processing software. It is seen from Figure 3a that QDs self-assemble to form a submonolayer film with few void places. The mean vertical size and mean lateral size of the QDs have been estimated from Figure 3 to be ~5.52 and ~8.0 nm, respectively, with a deviation of about 28%. More surprisingly, we cannot observe any QDs on the surface for samples with the LB ML number less than 8 by the STM measurements.

As one can see from the insets to Figure 1a,b, for the samples with a small ML number, QDs arrange in lines along step edges of the HOPG surface. It means that QDs can diffuse a rather long way before sticking on step edges. With an increase of the ML number, which leads to a steep rise of the QD density, the interacting QDs readily join to form clusters before reaching the step edges. As a result, randomly distributed QD arrays appear (see insets to Figures 2a,b and 3a).

In Figure 4, we depict a dependence of the QD density on the LB ML number (solid square), calculated on the basis of three 1 × 1 μm AFM images taken from different places on the substrate. This dependence consists of two regimes. For the LB ML number n no bigger than 3, the QD density (N_{QD}) changes as $N_{QD} = 9.1 \times 10^7 \times 10^{0.6n}$ cm^{-2}, whereas for the n larger

dx.doi.org/10.1021/jp206816f |J. Phys. Chem. C 2011, 115, 20148–20152

than 3, the dependence can be fitted by another function, namely, $N_{QD} = 1.3 \times 10^{10} \times 10^{0.1n}$ cm^{-2} (see solid lines in Figure 4). To explain such a dependence, a quantity of CdS molecules in a single quantum dot was estimated. We suggested that the QDs have a spherical shape. For this case, the quantity of CdS molecules in a single QD was calculated using the following expression

$$N_{CdS} = \alpha \cdot z \cdot \frac{\pi D^3}{6V_0} \quad (1)$$

where D is the diameter of a QD, V_0 is the volume of a conventional unit cell, and z is the number of CdS molecules in the conventional unit cell. The last parameter was calculated for an infinite crystal, in which all unit cells have neighbors. In a small QD, a considerable part of the cells located on the surface have no neighbor cells with some sides. The number of molecules z in such cells is larger, and the increase of z is taken into account by means of a factor α. The value of this coefficient α depends on the QD size and may be assumed to be 1.2 for QDs with a height of 3 nm and to be 1.1 for QDs with a height of 6 nm. The volume V_0 and the number z depend on the type of the crystal lattice structure. It is known that CdS in QDs exists in both zinc-blende and hexagonal wurtzite structures.[21] For bulk CdS, the volume of the conventional unit cell and the quantity of molecules in the cell are listed below:[22] for the zinc-blende structure, $V_0 = 196.93$ Å^3 and $z = 4$, whereas for the hexagonal wurtzite structure, $V_0 = 99.73$ Å^3 and $z = 2$. Substituting the above parameters in eq 1, we obtained that the N_{CdS} values are very similar for both of the two types of crystal structures. After multiplication of the N_{CdS} to the QD density, we can calculate the density of CdS molecules binding to form these QDs.

The calculated values are shown as open circles in Figure 4. For the estimation of the total density of CdS molecules in the LB matrix, the mean area for a single molecule in the LB ML was equally taken to be 0.4 nm^2.[19] This estimation gives that the density of CdS molecules is equal to 2.5×10^{14} per cm^2 in a single LB layer. This value increases linearly with an increase of the LB ML number (solid circles in Figure 4). As one can see for the LB ML number less than 4, the density of CdS molecules estimated from the QDs (open circles) is far smaller than that of the original CdS molecules in the LB matrix (closed circles in Figure 4). Therefore, at a small LB ML number, only a small part of CdS molecules form into QDs. With an increase of the LB ML number, the difference between the density of CdS molecules in the LB matrix and that of CdS molecules binding into QDs decreases. For the 20 LB ML sample, these densities are approximately equal within the estimation accuracy, and consequently, we can conclude that, for the 20 LB ML sample, almost all CdS molecules form into QDs. On the other hand, analyses of our previous data obtained by high-resolution transmission electron microscopy (TEM)[19,23] reveal that only a small part of CdS molecules belong to QDs before removing the LB matrix in the 20 ML sample. Indeed, the QD density in the LB matrix lies in the range between 1×10^{11} and 1×10^{12} cm^{-2} with a mean QD size of ~3 nm. Using eq 1, we found that a single CdS QD with such a diameter contains 340 molecules and, therefore, the average density of CdS molecules self-assembled into QDs is close to 1.8×10^{14} cm^{-2}. As indicated above, the density of CdS molecules in a single LB ML is equal to 2.5×10^{14} cm^{-2}. Consequently, the density of molecules in the 20 ML sample is equal to 5×10^{15} cm^{-2} and only $^1/_{10}$ of molecules bind to form QDs, whereas the rest of the molecules remain distributed separately in the LB matrix. Moreover, the TEM images of QDs arrays do not reveal any periodical spatial structure, which is considered as an evidence of the spinodal decomposition.[24] Therefore, we believe that the CdS molecules diffuse to bind into QDs due to a diffusion-limited aggregation. On the basis of the description of CdS QD self-assembly within the LB films developed in ref 18, we estimated the maximal size of QDs in the 20 ML samples to be no larger than 3 nm. Some overestimation can occur due to a possible increase of the QD size caused by the high-energy electron beam.[25] This size is close to that of the 1 and 2 LB ML samples in which CdS molecules move in the plane of the LB layer. It means that, during the formation of QDs in the LB matrix, CdS molecules move along the LB layers only, whereas interlayer diffusion is negligible. In the 4 and 8 LB ML samples, the average height of QDs is equal to 7 nm. The increase of the QD sizes after annealing leads to the red shift of a photoluminescence peak.[26] Growth of QDs after annealing of the thick LB ML samples may be due to diffusion of CdS molecules, moving across the LB layers. It should be noted that the estimated density of CdS molecules binding to QDs within the LB film is 1 order of magnitude higher than those obtained for 1−3 LB ML samples (see Figure 4). This could be due either to some QDs moving away during LB film thermal desorption or to the resolution limit for small QD observations. In the annealed samples with thick LB ML samples, bigger QDs attach to the substrate more strongly and, therefore, they are more easily detected.

The insets to Figures 1c and 2a,b demonstrate that QDs self-assemble into arrays. For the 3 LB ML sample, the arrays consist of a few dots. In the 4 and 8 LB ML samples, the clusters have a branched structure. The mean lateral size of the clusters strongly increases with the increasing ML number. Specifically, the typical lateral size of the QD clusters increases from 50 nm (4 ML) to 200 nm (8 ML). The absence of any free-standing QDs indicates that, at 200 °C, the QDs readily move over the substrate and aggregate to form clusters. From the density of QDs, we estimated a free path of QDs as an average distance between the centers of neighboring QDs. The free path is about 50 nm for the 4 ML sample. It should be noted that the lateral resolution of our AFM device is approximately equal to 15 nm; therefore, the discernible distance between neighboring QDs in the insets to Figure 2 is equal to ~15 nm.

For the 4 and 8 ML samples, the occurrence N as a function of the cluster aggregation number n are shown in Figure 2a,b. These distributions were obtained using three 1×1 μm AFM images. It is well known[27] that formation of clusters consisting of n QDs decreases a free energy of $E_n = (2n - 3)\alpha kT$, where the pair bond energy is $\varepsilon = \alpha kT$. We estimated parameters α by using the following expression for cluster occurrence from ref 27

$$N_n = N_0(N_1/N_0)^n \exp((2n - 3)\alpha) \quad (2)$$

where single, 2-, 3-, and n-QD clusters are denoted as N_1, N_2, N_3, and N_n, respectively, and N_0 is the total number of QDs. Usually at such analysis, monomers and dimers are omitted because of ease of sweeping by the AFM tip[11] or due to the limit of the image resolution.[27] In our case, monomers, dimers, and trimers were not used for estimation of α value as they obviously do not agree with eq 2 (see Figure 2a,b). By fitting the experimental data by eq 2, parameters N_3 and α were evaluated: $N_3 = 270$ and $\alpha = 0.83$ for the 4 LB ML sample, and $N_3 = 89$ and $\alpha = 1.53$ for the 8 LB

ML sample. The pair bond energies for annealing at 200 °C were found to be ε = 34 meV for the 4 LB ML sample and 62 meV for the 8 LB ML sample. The estimated values are close to the one reported for PbS QDs.[11,27] Meanwhile, the pair bond energy for the 8 LB ML sample is twice as large as that for the 4 LB ML sample. It can be explained as follows. Equation 2 is valid for the low-coverage case; that is, when an area of the free surface is much larger than the area covered by QDs, moreover QD clusters should be small. Most of the QD clusters in the 4 LB ML sample are relatively small, whereas in the 8 LB ML sample, the size of QD clusters increases due to the association with each other. Though, in the last sample, QDs cover a small part of the surface ($N_{QD} \cdot \pi \cdot R^2 \approx 3\%$), the density of the big QD clusters is large. Thus, eq 2 cannot be used to describe the situation.

Therefore, the existence of separate islands at low densities (1−3 ML), the ribbon structure at higher densities (4 and 8 ML), and complete coverage of the substrate surface with a further increase in density (20 ML) are very similar to previous investigations of QD self-assembling during solvent evaporation.[11,27] However, contrary to results of these works, in our samples, the QD density has no spatial periodicity, which is a feature of spinodal decomposition. The randomly aggregated clusters lead us to conclude that the clustering of QDs occurs due to diffusion-limited aggregation.

CONCLUSION

In this paper, the size, density, and spatial distribution of free-standing CdS QDs on the HOPG substrate formed by thermally induced desorption of the LB matrix with different thicknesses have been investigated. It was found that the ratio of CdS molecules binding into QDs increases from about 10% to 100% with increasing the LB ML number in the initial matrix from 3 to 20 ML. Separate QDs with mean sizes in the range between 1.7 and 1.9 nm were found after removing the matrix with a thickness of less than 3 ML. The size distribution of these QDs differs from that predicted by the generalized Lifshitz−Slezov theory. Starting from the 3 LB ML sample, QDs with a mean size of 5.5 nm begin to assemble into clusters. At last, when the thickness of the matrix reaches 20 MLs, a submonolayer film of QDs with rare ruptures completely cover the substrate. By analyzing occurrences of small clusters, pair bond energies of QDs were found to be 34 meV for the 4 LB ML sample and 62 meV for the 8 LB ML sample.

AUTHOR INFORMATION

Corresponding Author

*E-mail: protasov@thermo.isp.nsc.ru. Phone: +7-383-333-19-54. Fax: +7-383-330-90-29.

ACKNOWLEDGMENT

This work was supported by the Russian Foundation for Basic Research (grant no. 11-02-90427).

REFERENCES

(1) Hullavarad, N. V.; Hullavarad, S. S.; Karulkar, P. C. *J. Nanosci. Nanotechnol.* **2008**, *8*, 3272–3299.
(2) Hu, H. L.; Kung, S. C.; Yang, L. M.; Nicho, M. E.; Penner, R. M. *Sol. Energy Mater. Sol. Cells* **2009**, *93*, 51–54.
(3) Gubin, S. P.; Kataeva, N. A.; Khomutov, G. B. *Russ. Chem. Bull.* **2009**, *4*, 827–852.
(4) Ewins, C. T.; Stewat, B. *Thin Solid Films* **1996**, *284−285*, 49–52.
(5) Çapan, R.; Ray, A. K.; Hassan, A. K. *Thin Solid Films* **2007**, *515*, 3956–3961.
(6) Nabok, A. V.; Richardson, T.; Davis, F.; Charles, J. M. *Langmuir* **1997**, *13*, 3198–3201.
(7) Bagaev, E. A.; Zhuravlev, K. S.; Sveshnikova, L. L.; Badmaeva, I. A.; Repinskii, S. M.; Voelskow, M. *Semiconductors* **2003**, *37*, 1321–1325.
(8) Ou, Y. C.; Cheng, S. F.; Jian, W. B. *Nanotechnology* **2009**, *20*, 285401.
(9) Suzdalev, I. P.; Suzdalev, P. I. *Russ. Chem. Rev.* **2001**, *70*, 177–210.
(10) Bonn, D.; Otwinowski, J.; Sacanna, S.; Guo, H.; Wegdam, G.; Schall, P. *Phys. Rev. Lett.* **2009**, *103*, 156101.
(11) Tang, J.; Ge, G.; Brus, L. E. *J. Phys. Chem. B* **2002**, *106*, 5653–5658.
(12) Ge, G.; Brus, L. *J. Phys. Chem. B* **2000**, *104*, 9573–9575.
(13) Schmidt, S.; Hellweg, T.; von Klitzing, R. *Langmuir* **2008**, *24*, 12595–12603.
(14) Murray, C. B.; Kagan, C. R.; Bawendi, M. G. *Science* **1995**, *270*, 1335–1338.
(15) Shevchenko, E. V.; Talapin, D. V.; Kotov, N. A.; O'Brien, S.; Murray, C. B. *Nature* **2006**, *439*, 55–59.
(16) Narayanan, S.; Wang, J.; Lin, X.-M. *Phys. Rev. Lett.* **2004**, *93*, 135503.
(17) Lifshitz, I. M.; Slezov, V. V. *J. Phys. Chem. Solids* **1961**, *19*, 35–50.
(18) Nabok, A.; Iwantono; Ray, A.; Larkin, I.; Richardson, T. *J. Phys. D: Appl. Phys.* **2002**, *35*, 1512–1515.
(19) Repinskii, S. M.; Sveshnikova, L. L.; Khapov, Yu. I. *Russ. J. Phys. Chem. A* **1998**, *72*, 724–727.
(20) Yao, J. H.; Elder, K. R.; Guo, H.; Grant, M. *Phys. Rev. B* **1993**, *47*, 14110–14125.
(21) Rama Krishna, M. V.; Friesher, R. A. *J. Chem. Phys.* **1991**, *95*, 8309–8322.
(22) http://database.iem.ac.ru/mincryst/s_carta.php? GREENOCKITE.
(23) Milekhin, A. G.; Sveshnikova, L. L.; Repincki, S. M. *Phys. Solid State* **2002**, *44*, 1976–1980.
(24) Cahn, J. W. *J. Chem. Phys.* **1965**, *42*, 93–99.
(25) Nabok, A. V.; Ray, A. K.; Hassan, A. K. *J. Appl. Phys.* **2000**, *88*, 1333−1338.
(26) Bagaev, E. A.; Zhuravlev, K. S.; Sveshnikova, L. L.; Shcheglov, D. V. *Semiconductors* **2008**, *42*, 718–725.
(27) Ou, Y.-C.; Zhuravlev, K. S.; Fang, J.; Jian, W.-B. *J. Phys. Chem. C* **2010**, *114*, 17416–17421.